Electronic Supporting Information

Syntheses and structural characterization of the cobalt complexes

[Co(bztpen)Cl]BF_4 (3)
42.4 mg (0.1 mmol) bztpen and 23.8 mg (0.1 mmol) $CoCl_2$ x 6 H_2O were dissolved in 1 ml methanol. This solution was layered with a solution of 11.0 mg (0.1 mmol) $NaBF_4$ dissolved in 0.5 ml of methanol. Overnight purple block shaped crystals, suitable for X-ray analysis were formed. Calc. for $C_{27}H_{29}BClF_4CoN_5$: C, 53.62; H, 4.83; N, 11.58%. Found: C, 52.54; H, 4.83; N, 11.32% ESIMS (CH_3CN), *m/z* (%, assignment): 241.61 (55, $[Co(bztpen)]^{2+}$), 256.61 (40, $[Co(bztpen)Cl]^{2+}$), 518.17 (100, $[Co(bztpen)Cl]^{+}$).

[Co(metpen)Cl]SbF_6 (4)
104.2 mg (0.3 mmol) metpen and 66.6 mg (0.28 mmol) $CoCl_2$ x 6 H_2O were dissolved in 1 ml methanol and the resulting brown to violet solution was stirred for 15 min. 37.0 mg (0.14 mmol) $NaSbF_6$ dissolved in 1.5 ml MeOH were added. A purple powder was precipitated by adding the complex solution to diethyl ether. The solution was decanted and the precipitate was dried in air. Redissolving in acetone and diffusion of diethyl ether into this solution at room temperature yielded after 12 h purple single crystals, suitable for x-ray analysis. Calc. for $C_{21}H_{25}ClF_6CoN_5Sb$: C, 37.22; H, 3.72; N, 10.34%. Found: C, 37.13; H, 3.63; N, 10.57% ESIMS (CH_3CN), *m/z* (%, assignment): 203.08 (55, $[Co(metpen)]^{2+}$), 220.58 (40, $[Co(metpen)Cl]^{2+}$), 441.07 (100, $[Co(metpen)Cl]^{+}$).

[Co(bztpen)(OAc)]BPh_4 (5)
20.0 mg (0.05 mmol) bztpen and 11.2 mg (0.045 mmol) $Co(OAc)_2$ x 4 H_2O were dissolved in 1 ml methanol. A solution of 15.1 mg (0.044 mol) $NaBPh_4$ in 0.5 ml methanol was added. A precipitate was formed immediately, which was redissolved by adding 1.5 ml of dichloromethane. Salmon colored block shaped single crystals were obtained by diffusion of diethyl ether at room temperature after 12 h. $C_{53}H_{52}BCoN_5O_2$: C, 73.95; H, 6.09; N, 8.14%. Found: C, 73.18; H, 6.02; N, 7.78% ESIMS (CH_3CN), *m/z* (%, assignment): 241.61 (85, $[Co(bztpen)]^{2+}$), 527.12 (100, $[Co(bztpen)(HCO_2)]^{+}$), 517.16 (60, $[Co(bztpen)Cl]^{+}$).

Table S1 crystal and structure refinement data

	3	**4**	**5**
Empirical formula	$C_{27}H_{28}BClCoF_4N_5$	$C_{21}H_{25}ClCoF_6N_5Sb$	$C_{53}H_{52}BCoN_5O_2$
Formula weight	603.73	677.59	860.74
Crystal system	orthorhombic	orthorhombic	triclinic
Space group	Pbca	Pca2(1)	P-1
a/Å	16.309(3)	18.260(4)	13.234(3)
b/Å	17.791(4)	9.1630(18)	13.491(3)
c/Å	18.066(4)	15.057(3)	13.920(3)
α/°	90	90	96.33(3)
β/°	90	90	114.02(3)
γ/°	90	90	101.27(3)
V/ Å^3	5241.9(18)	2519.3(9)	2175.8(8)
Z	8	4	2
D_{calc}/g cm^3	1.530	1.787	1.314
T/K	193(2)	193(2)	193(2)
μ(MoK$_\alpha$)mm^{-1}	0.813	1.901	0.443
Crystal size/mm	0.36 x 0.36 x 0.48	0.53 x 0.38 x 0.04	0.38 x 0.30 x 0.50
F(000)	2480	1340	906
θ range/°	2.55 - 28.09	4.24 - 28.05	2.64 - 28.17
Index ranges	-21 ≤ h ≤ 20 -22 ≤ k ≤ 23 -23 ≤ l ≤ 23	-22 ≤ h ≤ 24 -10 ≤ k ≤ 12 -19 ≤ l ≤ 19	-17 ≤ h ≤ 17 -17 ≤ k ≤ 17 -18 ≤ l ≤ 17
Reflections collected	44894	20623	19812
Unique reflections	6334	6001	9719
R_{int}	0.0684	0.0573	0.0515
Refinement method	Full-matrix least-squares on F^2	Full-matrix least-squares on F^2	Full-matrix least-squares on F^2
Data/constraints/ parameters	6334 / 0 / 492	6001 / 1 / 330	9719 / 0 / 756
Goodness-of-fit on R^2	0.973	1.041	0.946
Final R indices[I > 2σ(I)]	R_1 = 0.0457 wR_2 = 0.1314	R_1 = 0.0357 wR_2 = 0.0940	R_1 = 0.0528 wR_2 = 0.1371
R indices (all data)	R_1 = 0.0622 wR_2 = 0.1449	R_1 = 0.0397 wR_2 = 0.0971	R_1 = 0.0856 wR_2 = 0.1560
Largest diff. peak/hole [e$^-$ Å^{-3}]	0.903 and -1.193	0.552 and -0.481	0.694 and -1.228

Table S2 Bond lengths [Å] and angles [°]

atoms	**3**	atoms	**4**	atoms	**5**
Co(1)-Cl(1)	2.3408(8)	Co(1)-Cl(1)	2.3271(10)	Co(1)-O(1)	2.041(3)
Co(1)-N(1)	2.189(2)	Co(1)-N(1)	2.203(3)	Co(1)-O(2)	2.783
Co(1)-N(2)	2.142(2)	Co(1)-N(2)	2.106(3)	Co(1)-N(1)	2.228(2)
Co(1)-N(3)	2.260(2)	Co(1)-N(3)	2.134(3)	Co(1)-N(2)	2.175(2)
Co(1)-N(4)	2.110(2)	Co(1)-N(4)	2.165(3)	Co(1)-N(3)	2.143(2)
Co(1)-N(5)	2.2093(19)	Co(1)-N(5)	2.267(3)	Co(1)-N(4)	2.243(2)
				Co(1)-N(5)	2.211(3)
				C(28)-O(1)	1.244(4)
				C(28)-O(2)	1.179(4)
Cal(1)-Co(1)-N(1)	171.41(6)	Cal(1)-Co(1)-N(1)	169.20(10)	O(1)-Co(1)-N(1)	152.82(10)
Cal(1)-Co(1)-N(2)	94.14(6)	Cal(1)-Co(1)-N(2)	103.34(9)	O(1)-Co(1)-N(2)	84.67(10)
Cl(1)-Co(1)-N(3)	88.77(6)	Cl(1)-Co(1)-N(3)	93.32(10)	O(1)-Co(1)-N(3)	92.90(10)
Cal(1)-Co(1)-N(4)	103.78(7)	Cal(1)-Co(1)-N(4)	104.58(10)	O(1)-Co(1)-N(4)	127.38(11)
Cl(1)-Co(1)-N(5)	102.73(6)	Cal(1)-Co(1)-N(5)	89.03(9)	O(1)-Co(1)-N(5)	90.16(11)
N(1)-Co(1)-N(2)	77.58(8)	N(1)-Co(1)-N(2)	75.31(14)	N(1)-Co(1)-N(2)	73.48(9)
N(1)-Co(1)-N(3)	99.76(8)	N(1)-Co(1)-N(3)	76.82(15)	N(1)-Co(1)-N(3)	76.52(9)
N(1)-Co(1)-N(4)	76.24(8)	N(1)-Co(1)-N(4)	81.13(13)	N(1)-Co(1)-N(4)	79.27(9)
N(1)-Co(1)-N(5)	80.68(7)	N(1)-Co(1)-N(5)	101.36(14)	N(1)-Co(1)-N(5)	103.66(10)
N(2)-Co(1)-N(3)	170.70(8)	N(2)-Co(1)-N(3)	104.22(13)	N(2)-Co(1)-N(3)	102.11(9)
N(2)-Co(1)-N(4)	102.99(8)	N(2)-Co(1)-N(4)	144.33(13)	N(2)-Co(1)-N(4)	141.57(9)
N(2)-Co(1)-N(5)	96.08(8)	N(2)-Co(1)-N(5)	83.02(12)	N(2)-Co(1)-N(5)	85.30(10)
N(3)-Co(1)-N(4)	84.84(7)	N(3)-Co(1)-N(4)	95.89(12)	N(3)-Co(1)-N(4)	97.21(8)
N(3)-Co(1)-N(5)	74.64(7)	N(3)-Co(1)-N(5)	171.62(13)	N(3)-Co(1)-N(5)	172.21(9)
N(4)-Co(1)-N(5)	145.89(8)	N(4)-Co(1)-N(5)	75.74(13)	N(4)-Co(1)-N(5)	75.28(9)

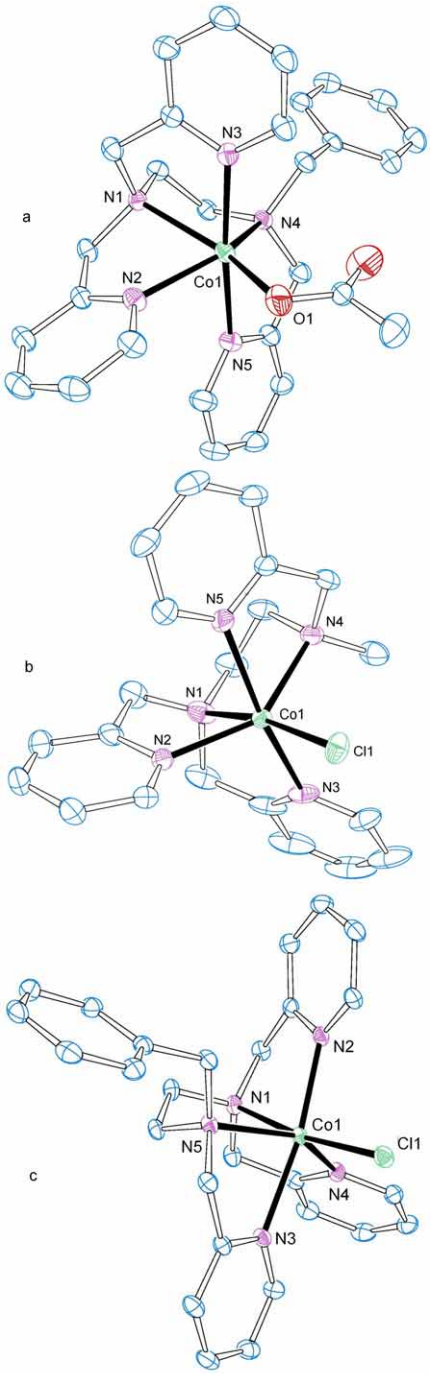

Fig. S1 Ortep plot of the complex cations (a) $[Co(bztpen)Cl]^+$ (**3**) (b) $[Co(metpen)Cl]^+$ (**4**) and (c) $[Co(bztpen)OAc]^+$ (**5**). The thermal ellipsoids are shown at 30% probability. Hydrogen atoms are omitted for clarity.

Kinetic analysis:

Oxidation of [Fe(bztpen)Cl]ClO_4

Table S3: Observed rate constants, k_{obs} (s^{-1}), for the oxidation reaction of [Fe(bztpen)Cl]ClO_4 with H_2O_2 in methanol calculated from absorbance vs. time traces at 393 nm. Each rate constant is the average of at least three kinetic runs.

$[H_2O_2]$ [M]	-40°C	-35°C	-30°C	-25°C
0.01	0.19 ± 0.02	0.46 ± 0.04	0.8 ± 0.2	0.1 ± 0.1
0.05	0.63 ± 0.02	0.95 ± 0.03	1.47 ± 0.09	2.3 ± 0.1
0.10	1.05 ± 0.02	1.70 ± 0.05	2.43 ± 0.08	4.3 ± 0.1
0.16	1.59 ± 0.04	2.3 ± 0.1	3.4 ± 0.1	5.6 ± 0.2
0.25	1.59 ± 0.06	2.5 ± 0.1		
0.375	1.9 ± 0.2	2.8 ± 0.2		
0.50	2.0 ± 0.4	3.5 ± 0.4	5.4 ± 0.1	10.3 ± 0.3
0.75	2.5 ± 0.5	4.6 ± 0.4	6.2 ± 0.1	15.1 ± 0.5
1.00	3.1 ± 0.5	5.8 ± 0.5	8.2 ± 0.2	16.3 ± 0.5
1.50	3.6 ± 0.3			

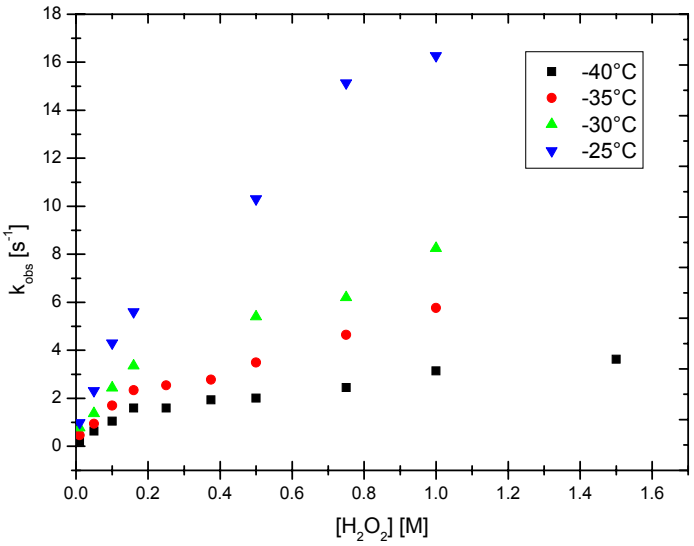

Figure S2: k_{obs} versus $[H_2O_2]$ for the oxidation of [Fe(bztpen)Cl]ClO_4 by H_2O_2 in methanol.

Table S4: Second order rate constants for the oxidation of [Fe(bztpen)Cl]ClO_4 by hydrogen peroxide in methanol calculated from the initial slopes of the curved data plots in Figure 1 as plotted in Figure 2.

Temp. [°C]	k [$M^{-1} s^{-1}$]	Intercept [s^{-1}]
-40°C	9.2 ± 0.3	0.13 ± 0.03
-35°C	12.8 ± 0.6	0.34 ± 0.06
-30°C	17.6 ± 0.9	0.57 ± 0.08
-25°C	31 ± 3	0.8 ± 0.3

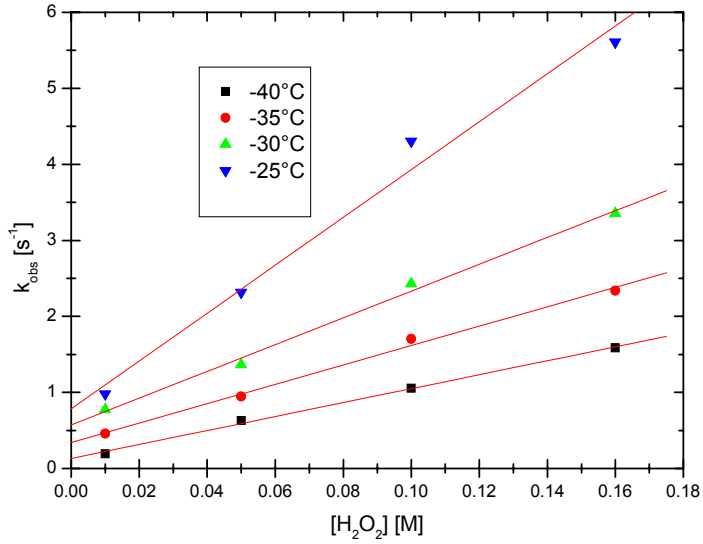

Figure S3: k_{obs} *vs.* [H_2O_2] to calculate the initial slopes and intercepts of the curved plots in Figure 1.

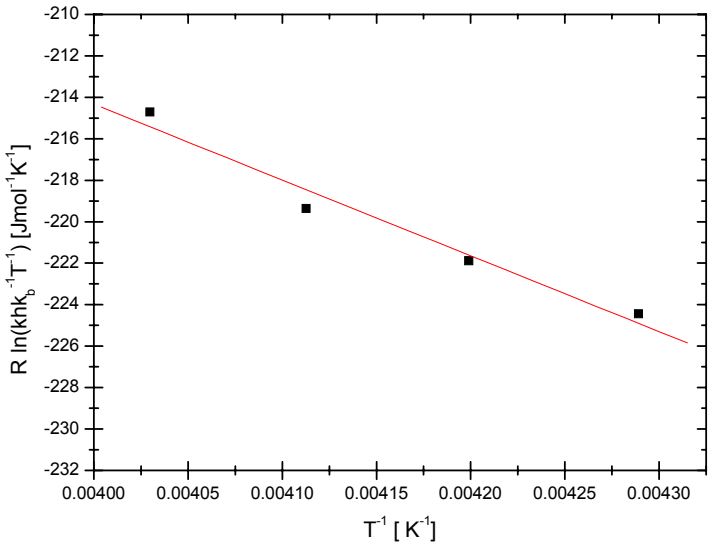

Figurre S5: "Eyring plot" for the oxidation of [Fe(bztpen)Cl]ClO_4 in methanol.

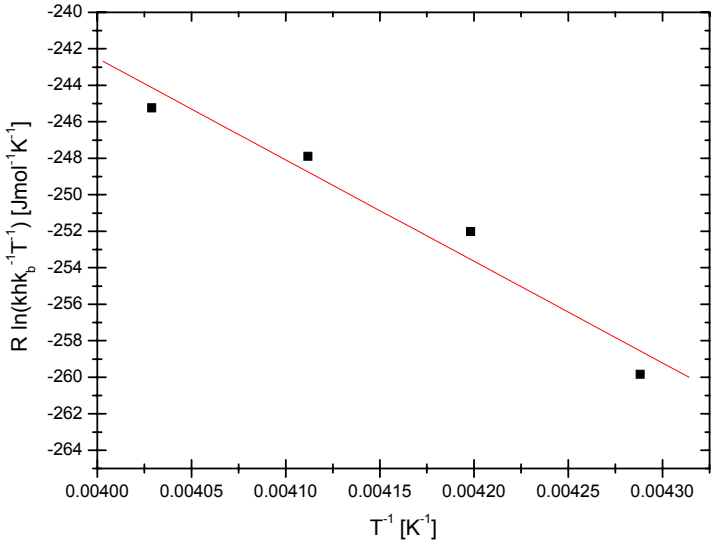

Figure S6: "Eyring plot" for the back reaction of the oxidation of [Fe(bztpen)Cl]ClO_4 in methanol.

Table S5: Activation parameters for the oxidation reaction of [Fe(bztpen)Cl]ClO_4 in methanol calculated from the "Eyring plots" in Figure 3 and Figure 4.

	$\Delta H^{\ddagger}$ [kJ mol^{-1}]	$\Delta S^{\ddagger}$ [J mol^{-1} K^{-1}]
	37 ± 5	-68 ± 20
Back reaction	56 ± 9	(-19 ± 37)

The $\Delta S^{\ddagger}$ value for the back reaction has no meaning due to the large error limits, which are normal for calculations from intercepts.

Formation of $[Fe(bztpen)OOH]^{2+}$

Table S6: Observed rate constants, k_{obs} (s^{-1}), for the reaction of the formation reaction of $[Fe(bztpen)OOH]^{2+}$ in methanol calculated from absorbance *vs.* time traces at 550 nm. Each rate constant is an average of at least three measurements.

$[H_2O_2]$ [M]	20°C	25°C	30°C	35°C	40°C
0.01	0.0268 ± 0.0001	0.0380 ± 0.0001	0.0575 ± 0.0002	0.0856 ± 0.0003	0.1316 ± 0.0005
0.02	0.0365 ± 0.0001	0.0526 ± 0.0002	0.0800 ± 0.0002	0.1173 ± 0.0004	0.1805 ± 0.0004
0.04	0.0662 ± 0.0002	0.0927 ± 0.0002	0.1290 ± 0.0004	0.1830 ± 0.0004	0.2725 ± 0.0008
0.06	0.0873 ± 0.0002	0.1230 ± 0.0003	0.1772 ± 0.0004	0.2595 ± 0.0006	0.3643 ± 0.0008
0.08				0.3433 ± 0.0007	0.482 ± 0.001

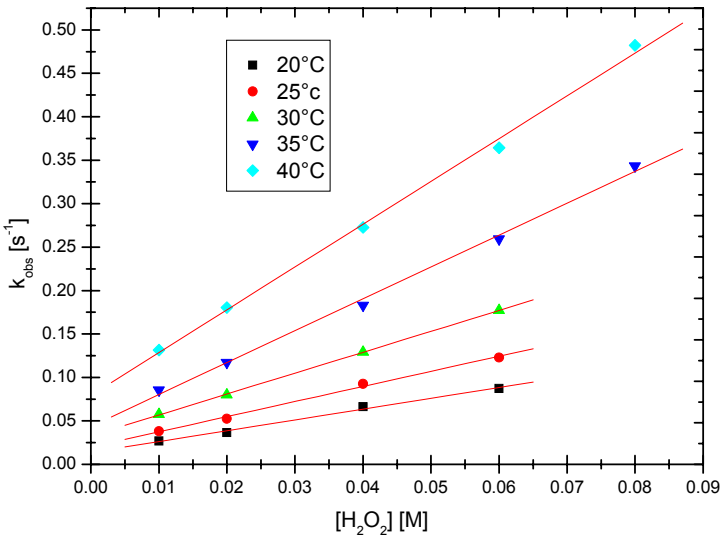

.

Figure S6:k_{obs} *vs.* $[H_2O_2]$ for the formation of $[Fe(bztpen)OOH]^{2+}$

Table S7: Second order rate constants for the formation reaction of the iron(III) hydroperoxido complex with H_2O_2 in methanol calculated from slope of the straight lines.

Temp. [°C]	k [M^{-1} s^{-1}]	Intercept [s^{-1}]
20	1.24 ± 0.07	0.014 ± 0.003
25	1.74 ± 0.08	0.020 ± 0.003
30	2.41 ± 0.01	0.0328 ± 0.0007
35	3.7 ± 0.1	0.044 ± 0.006

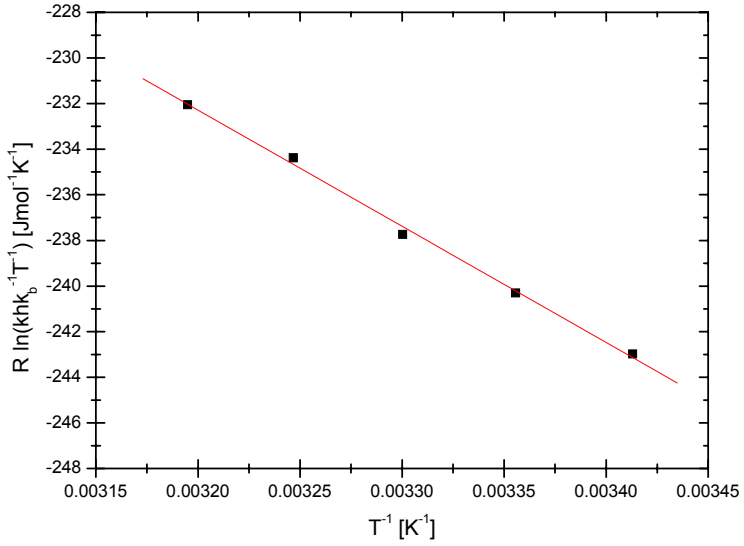

Figure S7: "Eyring plot" for the formation of $[Fe(bztpen)OOH]^{2+}$.

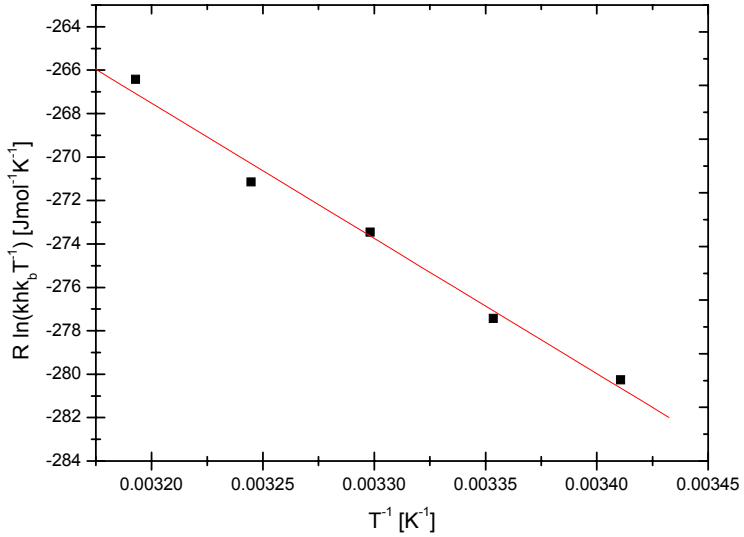

Figure S8: "Eyring plot" for the back reaction of the formation of $[Fe(bztpen)OOH]^{2+}$.

Table S8: Activation parameters for the formation reaction of hydroperoxido complex in methanol calculated from the "Eyring plots" in Figure 6 and Figure 7.

	$\Delta H^{\ddagger}$ [kJ mol^{-1}]	$\Delta S^{\ddagger}$ [J mol^{-1} K^{-1}]
	51 ± 2	-69 ± 5
Back reaction	62 ± 4	-68 ± 13

High pressure kinetics

Table S9: Observed rate constants, k_{obs} (s^{-1}) , for the formation of $[Fe(bztpen)OOH]^{2+}$ in methanol under high pressure conditions at 27 °C calculated from absorbance *vs.* time traces at 550 nm. Each rate constant is an average of at least three measurements.

$[H_2O_2]$ [M]	100 MPa	500 MPa	800 MPa	1100 MPa	1300 MPa
0.053	0.090	0.090	0.080	0.090	
0.080	0.128	0.125	0.123		0.122
0.106	0.171	0.166	0.163		0.152
0.133	0.193	0.197	0.188	0.199	0.192

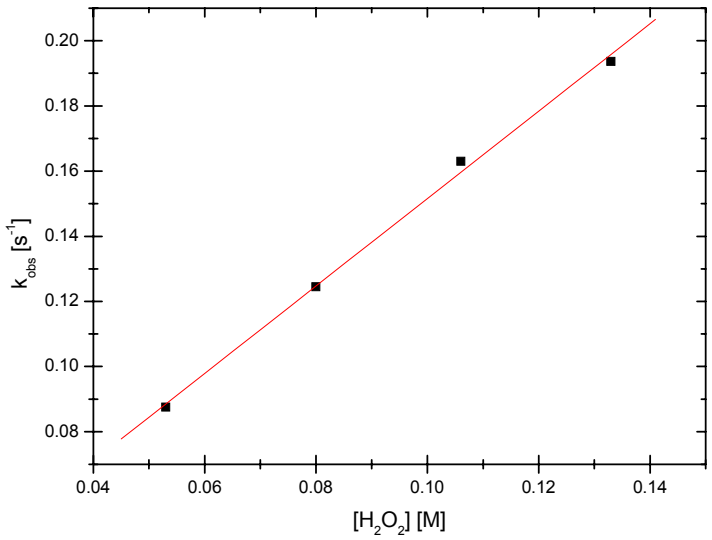

Figure S9: k_{obs} *vs.* $[H_2O_2]$ for the formation of $[Fe(bztpen)OOH]^{2+}$ under high pressure conditions at 27°C (data point are average values over all pressures).

Table S10: Second order rate constants for the formation of $[Fe(bztpen)OOH]^{2+}$ with H_2O_2 in methanol under high pressure conditions calculated from the straight line.

Temp. [°C]	k [M^{-1} s^{-1}]	Intercept [s^{-1}]
27	1.34 ± 0.05	0.0017 ± 0.0005